

# Testing Models for IMF Variation in Milky Way-like Galaxies

Dávid Guszejnov<sup>1</sup>★, Philip F. Hopkins<sup>1</sup> and Xiangcheng Ma<sup>1</sup>

<sup>1</sup> *TAPIR, MC 350-17, California Institute of Technology, Pasadena, CA 91125, USA*

To be submitted to MNRAS, 13 December 2024

## ABSTRACT

One of the key observations regarding the stellar initial mass function (IMF) is its near-universality in the Milky Way (MW), which provides a powerful way to test different star formation models that predict the IMF. However, those models are almost universally “cloud-scale” or smaller – they take as input or simulate single molecular clouds (GMCs), clumps, or cores, and predict the resulting IMF as a function of the cloud properties. Without a model for the progenitor properties of all clouds which formed the stars at different locations in the MW (including ancient stellar populations formed in high-redshift, likely gas-rich dwarf progenitor galaxies that looked little like the Galaxy today), the predictions cannot be explored. We therefore utilize a high-resolution fully-cosmological simulation (from the Feedback In Realistic Environments project), which forms a MW-like galaxy with reasonable mass, morphology, abundances, and star formation history, and explicitly resolves massive GMCs; we combine this with several cloud-scale IMF models applied independently to *every star-forming resolution element* in the simulation to synthesize the predicted IMF variations in the present-day galaxy. We specifically explore broad classes of models where the IMF depends on the Jeans mass, the sonic or “turbulent Bonner-Ebert” mass, fragmentation with some polytropic equation-of-state, or where it is self-regulated by protostellar feedback. We show that all of these models, except the feedback-regulated models, predict far more variation ( $\sim 0.6 - 1$  dex  $1\sigma$  scatter in the IMF turnover mass) than is observed in the MW. This strongly constrains the parameters that can drive IMF variation in nearby galaxies, as well.

**Key words:** stars: formation – turbulence – galaxies: star formation – cosmology: theory

## 1 INTRODUCTION

The (instantaneous) mass distribution of stars at their formation time, also known as the initial mass function (IMF), is one of the key predictions of any star formation model. This governs essentially all observable and theoretical aspects of star formation and stellar populations – observable luminosities and colours; effects on stellar environments via feedback in the form of stellar winds, radiation, supernovae; nucleosynthesis and galactic chemical evolution, and so on. The IMF has been well-studied within the MW, and appears to be well-fit by a simple function with a [Salpeter \(1955\)](#) power-law slope at high masses and lognormal-like turnover at low masses ([Chabrier 2005](#); [Kroupa 2002](#)). Perhaps the most interesting feature of the IMF is its universality: it has been found that there is little or no variation within the MW (for recent reviews, see [Chabrier 2003](#); [Bastian et al. 2010](#); [Offner et al. 2014](#); [Krumholz 2014](#), and references therein), albeit with a few possible outliers (e.g. [Luhman et al. 2009](#); [Kraus et al. 2017](#)). As [Offner et al. \(2014\)](#) emphasize, this universality includes both very young ( $\sim$  Myr-old) and very old ( $\sim 10$  Gyr-old) stellar populations; stars forming in small, nearby GMCs with masses  $\sim 10^4 - 10^6 M_\odot$  and massive complexes with masses  $\sim 10^6 - 10^7 M_\odot$ ; the solar neighbourhood at  $\sim 10$  kpc from the galactic centre (where the gas disk surface density is  $\sim 10 M_\odot \text{pc}^{-2}$ ) and the central molecular zone

at sub-kpc and  $\sim 100$  pc scales (where gas surface densities are order-of-magnitude larger).

In other galaxies, the IMF usually must be *assumed*, and with an IMF assumption, physical properties of the stellar populations and galaxies (e.g. their stellar masses) are derived from observables (e.g. light, colours). This makes it critical to understand galaxy formation. However, the universality of the IMF in old stellar populations in the MW makes it likely it is near-universal in other galaxies as well, since older populations in the MW formed when the galaxy was much younger, likely a typical, high-redshift, gas-rich, metal-poor dwarf galaxy. There are indirect constraints both from spectral features and integrated mass-to-light constraints in nearby galaxies: these mostly also favor a universal IMF (e.g. [Fumagalli et al. 2011](#); [Koda et al. 2012](#); [Andrews et al. 2013, 2014](#); [Weisz et al. 2015](#)). More recently there have been more interesting hints of variation in the centres of massive elliptical galaxies ([van Dokkum & Conroy 2010, 2011](#); [Conroy & van Dokkum 2012](#); [Treu et al. 2010](#); [Sonnenfeld et al. 2015](#); [Cappellari et al. 2012](#); [Posacki et al. 2015](#); [Martín-Navarro et al. 2015b,a,c](#)), and perhaps also in faint dwarf galaxies ([Hoversten & Glazebrook 2008](#); [Brown et al. 2012](#); [Geha et al. 2013](#)). Even so, it is worth stressing that the implied variation is not radical: it implies variation of a factor  $< 2$  in the stellar mass-to-light ratio.

A number of IMF models have been proposed that allow variations (e.g. [Baugh et al. 2005](#); [Hopkins 2013](#); [Davé et al. 2012](#); [Narayanan & Davé 2012](#)). More recently, the hints of galaxy-to-galaxy variation discussed above have prompted a

★ E-mail: [guszejnov@caltech.edu](mailto:guszejnov@caltech.edu)

new wave of theoretical models seeking to explain IMF variations in different galaxies (e.g. Weidner et al. 2013; Bekki 2013; Chabrier et al. 2014; Ferreras et al. 2015). However, these models in every case rely on very strong simplifying assumptions – the IMF is predicted as a function of the cloud properties out of which the stars form, such as its temperature, density, turbulent velocity dispersion, virial parameter, etc. (from which properties like the Jeans mass, or the turbulent Bonner-Ebert mass, or the IGIMF turnover mass, are determined). These cannot be known for all the clouds that formed the old stellar populations present today in a galaxy (or even for most clouds within a galaxy) so instead some strong additional assumptions are applied, for example assuming isothermal gas with  $T = 10$  K, or a constant sonic mass/length or Jeans mass. But if these properties vary cloud-to-cloud, as they do even at present day in the MW, then the models can be tested. It *must* be the case that a model for extragalactic variation based on, say, mean variations in gas density, produces variations *within the MW* based on that same physical property that fall within observational limits.

In this paper we investigate the variation of the IMF peak (imprinted by this additional physics) in a number of IMF models, by combining a high-resolution simulation of a MW-like galaxy (where the cloud-scale properties can be resolved) with the relevant small-scale models for IMF variation as a function of cloud properties.

## 2 MODEL AND METHODOLOGY

### 2.1 Simulation

We utilize a set of numerical simulations MW-like galaxies (see Table 1) presented in Hopkins et al. (2017), from the Feedback in Realistic Environments (FIRE) project (Hopkins et al. 2014).<sup>1</sup> The simulations are fully cosmological “zoom-in” simulations (where resolution is concentrated on one galaxy in a large cosmological box, run from redshift  $z > 100$  to today) and are run using GIZMO (Hopkins 2015)<sup>2</sup>, with the mesh-free Godunov “MFM” method for the hydrodynamics (Hopkins 2015). Self-gravity is included with fully-adaptive force and hydrodynamic resolution; the simulation mass resolution is fixed at 7000 or 56000  $M_\odot$  (Table 1). The simulations include detailed metallicity-dependent cooling physics from  $T = 10 - 10^{10}$  K, including photo-ionization/recombination, thermal bremsstrahlung, Compton, photoelectric, metal line (following Wiersma et al. 2009), molecular, fine structure (following Ferland et al. 2013), dust collisional and cosmic ray processes, including both a meta-galactic UV background and each star in the simulation as a local source.

Individual stars are not resolved in the simulations; but star formation is approximated from resolved scales via a sink-particle method. Gas which is locally self-gravitating, self-shielding, Jeans unstable, and exceeds a minimum density  $n > 100 - 1000 \text{ cm}^{-3}$  (Table 1) is transformed into “star cluster sink particles” on its dynamical time. Each such particle represents an IMF-averaged single stellar population of

the same age and metallicity, with mass equal to the mass resolution.

Once formed, the simulations include feedback from these star particles via OB & AGB mass-loss, SNe Ia & II, and multi-wavelength photo-heating and radiation pressure; with inputs taken directly from stellar evolution models (Leitherer et al. 1999), assuming (in-code) a universal IMF (Kroupa 2002).

The reason for using cosmological simulations instead of present-day observational data or a more localized cloud simulation is that stars at a given present-day position in a galaxy can form at wildly different times/places (some even in other dwarf galaxies). This makes it impossible to assign the properties of their progenitor clouds (needed for the IMF models) from observations (or localized simulations) alone. Note that this also means that the progenitor cloud properties are meant “at formation” which may be at a much earlier time and at a very different place than the present day position of the star particle.

The galaxies studied here – especially our “case study” example, **m12i** (shown in Fig. 1) – have been studied extensively in previous work: they are similar to the MW in its stellar mass, present-day gas fraction and SFR (Hopkins et al. 2014), metallicity (Ma et al. 2016b), stellar kinematics, thin+thick disk morphology, metallicity gradient and metal abundance ratio gradients (in both vertical and radial directions) and stellar age distribution (Ma et al. 2016a, 2017),  $R$ -process element distribution (van de Voort et al. 2015), and galactic stellar halo and satellite dwarf population (Wetzel et al. 2016). These and other FIRE simulations have been shown to reproduce the observed Kennicutt-Schmidt relation (Sparre et al. 2015; Orr et al. 2017), properties of galactic outflows (Muratov et al. 2015), and (in higher resolution, non-cosmological simulations) the observed mass function (and CO luminosities), size-mass, and linewidth-size distribution of GMCs (Hopkins et al. 2012, 2013). One might reasonably worry that at the lower resolution necessary in cosmological simulations, this cannot be captured; therefore in Fig. 2 we plot the mass function and linewidth-size relation of GMCs identified at present-day in the actual simulations studied here. They appear to agree at least plausibly with the observed properties (Dobbs et al. 2014; Heyer & Dame 2015). All of this is not to say that the simulations are perfect analogues to the MW; however they are at least a reasonable starting point (see Fig. 2 for comparisons).

Our analysis mainly focuses on the galaxy **m12i** (Fig. 1; see Wetzel et al. 2016; Hopkins et al. 2017) whose mass resolution is too low to resolve smaller GMCs but – due to the shape of the GMC mass function – most of the mass is concentrated in much larger GMCs which are resolved (Fig. 2). Also, our choice of  $n_{\text{crit}} = 100 - 1000 \text{ cm}^{-3}$  (at mass resolution 7000 – 56000  $M_\odot$ ) can be justified by assuming that GMCs follow the mass-size relation of Bolatto et al. (2008) ( $M_{\text{cloud}} \sim \pi (85 M_\odot \text{ pc}^{-2}) R_{\text{cloud}}^2$ ), which implies the density threshold for star formation is higher than the mean density of resolved clouds. More specifically, we chose the density threshold to correspond to the typical density where the Jeans/Toomre fragmentation scale falls below our mass resolution. In either case the GMC mass function and SFR is dominated by the most massive (hence well-resolved) clouds. This is evident in Fig. 2, where we show the GMC mass function and linewidth-size relation predicted at present-day in

<sup>1</sup> <http://fire.northwestern.edu>

<sup>2</sup> <http://www.tapir.caltech.edu/~phopkins/Site/GIZMO.html>

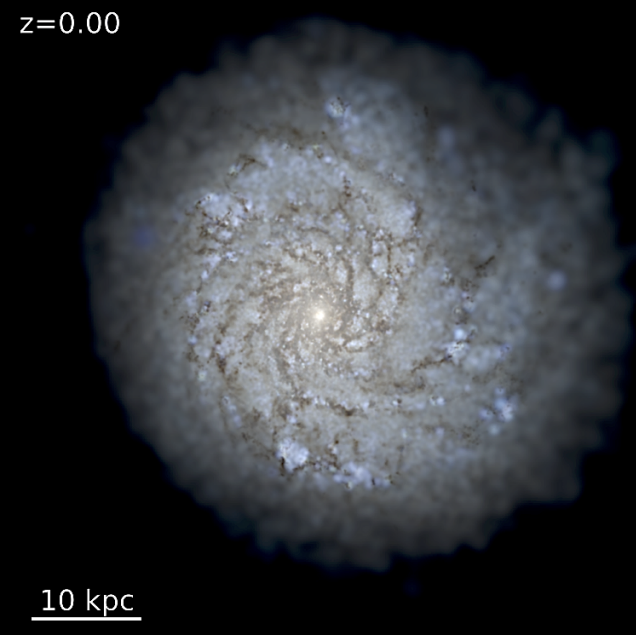


**Figure 1.** Visualization of the starlight (mock *ugr* composite image, accounting for each stellar sink-particle’s age and metallicity and ray-tracing including dust obscuration) from one of the simulated MW-like galaxies (see Table 1) we use in our calculations (galaxy **m12i** from Hopkins et al. 2017). Note that resolved molecular clouds and arms are evident.

the galaxy both (a) agree well with observations, and (b) are insensitive to resolution (except, of course, that at higher resolution they extend to smaller GMCs). This gives us some confidence that our predictions are not strongly resolution-dependent. In Table 1 we show the ultimate effects of varying resolution and  $n_{\text{crit}}$  as well as physics (in an otherwise identical run including magnetic fields, **m12i+MHD**). These do not significantly alter our predictions.

Because the simulations resolve down to cloud scales, but no further, we will treat each star-forming gas element as an independent “parent cloud”, which sets the initial conditions for its own detailed IMF model. Specifically, whenever a sink particle is spawned, we record all properties of the parent gas element from which it formed, and use these in post-processing to predict the IMF. Fig 3 shows the density and temperature distribution of these “star forming particles” (gas at the moment the simulation assigned its mass to a sink particle) at the time of their formation, from our low-resolution **m12i** run. Not surprisingly most sinks form around the simulation density threshold from this particular run ( $\sim 100 \text{ cm}^{-3}$ ). Note that this is not the density/temperature of the gas that which directly collapses and forms stars, instead these are the properties of the progenitor molecular clouds which will (and must, physically) fragment into denser sub-clumps that can directly form stars.

## 2.2 From Parent Cloud to IMF Properties

From this point we infer the IMF turnover mass from the initial conditions of these parent clouds. This exercise has been done in detail by Guszejnov et al. (2016) where the semi analytical framework of Guszejnov & Hopkins (2016) was utilized to create a mapping between GMC properties and the IMF. Fig. 4 shows how the IMF peak scales with initial temperature in an equation of state (EOS) and a pro-

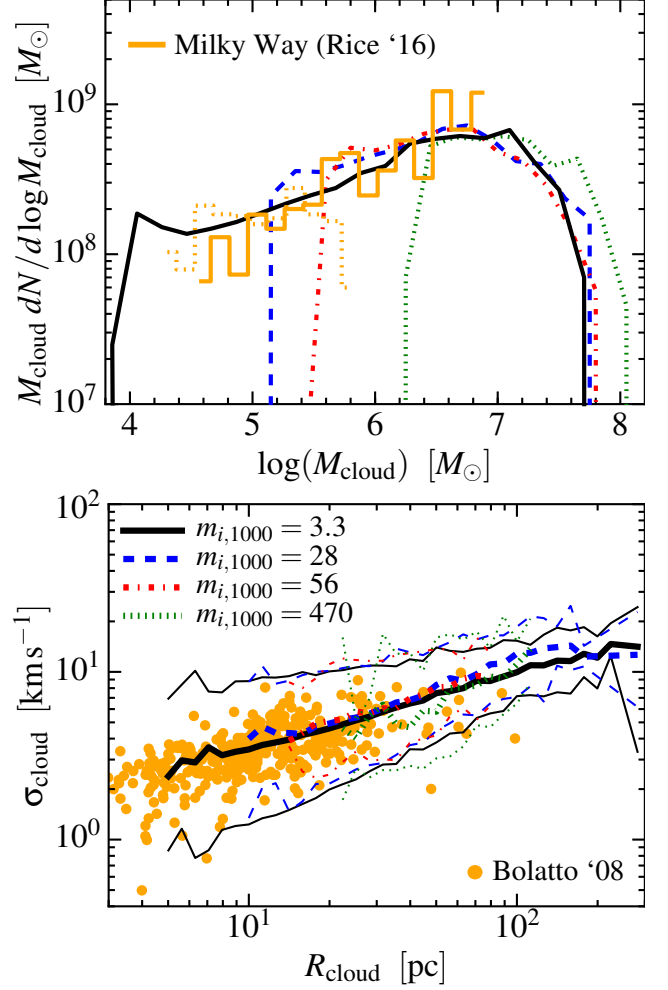


**Figure 2.** *Top:* Mass function (MF) of GMCs in the fiducial simulation (Fig. 1) at  $z \approx 0$ , at different mass resolution (baryonic particle mass  $m_i = 1000 m_{i,1000} M_\odot$ ). We restart the fiducial simulation from Fig. 1 (with  $m_{i,1000} = 56$ ) at  $z = 0.1$ , after re-sampling the particles to raise/lower the mass resolution. We then evolve it for  $\sim 1$  Gyr to  $z = 0$ , and measure the MF of dense cold-gas clouds (identified in post-processing with a friends-of-friends group-finder) time-averaged over the last  $\sim 100$  Myr inside  $< 20$  kpc of the galaxy center. All details of the resampling and group-finding method are in Hopkins et al. (2017). We compare the observed MW GMC MF from Rice et al. (2016), normalized to the same total mass, measured inside (*solid*) and outside (*dotted*) the solar circle. At all resolutions, a GMC MF similar to that observed is recovered. The most massive GMCs contain most of the mass/star formation and are the first-resolved. At higher resolution we extend to smaller GMCs. *Bottom:* Linewidth-size relation for the same clouds (median in thick lines; 5 – 95% intervals in thin lines), vs. the MW and nearby-galaxy compilation in Bolatto et al. (2008) (note our definition of  $R_{\text{cloud}}$  is equivalent to their  $\sigma_r$ ). Agreement is good. There is no systematic resolution dependence (other than sampling smaller clouds at higher resolution).

tostellar feedback based IMF model. Such scaling relations can be analytically derived for other IMF models (e.g. Jeans mass) as well – we focus here on how each model predicts the turnover or “critical” mass  $M_{\text{crit}}$  scale, since this is the most identifiable feature of the IMF (it sets the mass-to-light ratio, and varies significantly between models). In contrast the bright-end slope varies negligibly between models, so is not useful as a diagnostic.

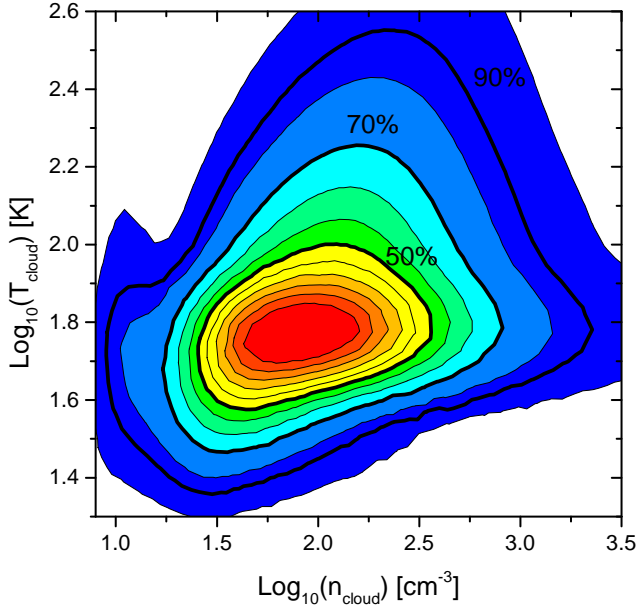


**Figure 3.** Density map of the distribution of star forming clouds (gas elements which formed a stellar sink particle in the galaxy simulation, *at the moment of sink formation*) in density and temperature space, in our example low-resolution **m12i** simulation (mass  $56000 M_{\odot}$ ) from Table 1. The plot is normalized so that the distribution integrates to unity, the contours corresponding to 50, 70 and 90% of clouds are drawn with thick black lines. Note that because this is a Lagrangian code, sink particles always form at a fixed cloud *mass* scale (equal to our resolution) and the location of the peak is set by our choice of  $n_{\text{crit}}$  ( $\sim 100 \text{ cm}^{-3}$  here). This choice, however, does not affect the relevant part of this result, namely the scatter in both  $n_{\text{cloud}}$  and  $T_{\text{cloud}}$  which translates to scatter in the local IMF and is insensitive to our choice of  $n_{\text{crit}}$  (see Table 1). If we compare one of the higher-resolution simulations in Table 1, the centroid of the diagram moves to  $n_{\text{cloud}} \sim n_{\text{crit}} \sim 1000 \text{ cm}^{-3}$ , and  $T \sim 30 \text{ K}$  (with 90% of the gas at  $n_{\text{cloud}} > 1000 \text{ cm}^{-3}$  having a temperature  $T < 80 \text{ K}$ , consistent with the high-density tail of the low-resolution run here). Note that Narayanan & Hopkins (2013) show the inferred temperature scatter from mock CO-ladder observations will tend to be significantly smaller than the scatter plotted here.

In this paper we investigate the sensitivity to initial conditions for the following classes of IMF models (summarized in Table 1):

- **Jeans mass models:** Since the Jeans instability is the primary mechanism for the collapse of gas clouds into stars, these models assume that IMF properties are set by local mean Jeans mass of the parent molecular cloud complex (e.g. Bate & Bonnell 2005). Therefore, the critical mass is

$$M_{\text{crit,J}} \sim \frac{\pi c_s^3}{6G^{3/2}\rho^{1/2}}. \quad (1)$$

Note that the models may still assume sub-fragmentation to smaller scales, but the key assumption (for our purposes) is simply that the turnover mass somehow scales proportional to the parent cloud Jeans mass.

- **Opacity limit equation of state (EOS) models:** As the molecular gas becomes denser it reaches the point where it becomes opaque to its own cooling radiation, leading to a transition from isothermal to adiabatic behavior, terminating fragmentation at the Jeans mass at this density. This can

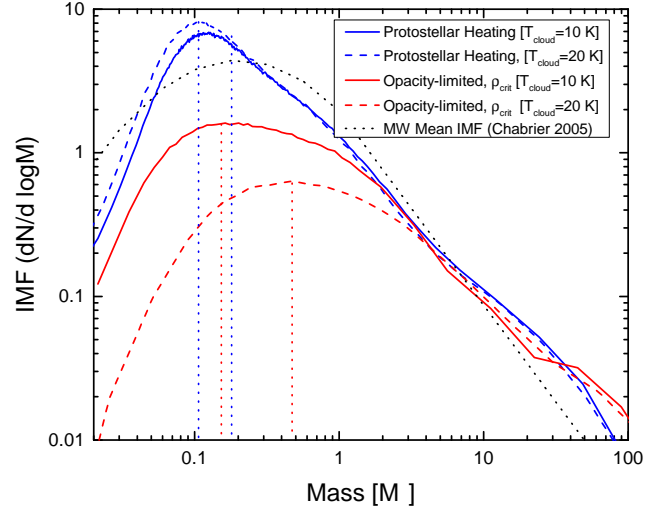


**Figure 4.** Predicted IMF using the framework of Guszejnov & Hopkins (2016), within progenitor clouds with different initial temperatures  $T_{\text{cloud}} = 10 \text{ K}$  or  $20 \text{ K}$ . We compare two IMF models from Table 1: (1) accounting for proto-stellar heating, and (2) ignoring heating and treating the gas with a polytropic equation-of-state until some it reaches the opacity limit. We compare the standard fit to the observed IMF from Chabrier (2005). Differences in temperature produce different model shifts, per the scalings in Table 1. occur at a critical volume density  $\rho_{\text{crit}}$  (e.g. Low & Lynden-Bell 1976; Whitworth et al. 1998; Larson 2005; Glover & Mac Low 2007; Jappsen et al. 2005; Masunaga & Inutsuka 2000). Motivated by radiation transfer simulations like Bate 2009 we also investigated the case where the transition occurs at a critical surface density  $\Sigma_{\text{crit}}$ . The critical masses in these cases are:

$$M_{\text{crit},\rho} \sim \frac{\pi c_s^3}{6G^{3/2}\rho_{\text{crit}}^{1/2}}, \quad M_{\text{crit},\Sigma} \sim \frac{c_s^4}{G^2\Sigma_{\text{crit}}}, \quad (2)$$

where  $\rho_{\text{crit}}$  and  $\Sigma_{\text{crit}}$  are the critical densities for the isothermal-adiabatic transition.

- **Turbulent/sonic mass models:** A number of analytical theories derive the CMF and IMF from the properties of the turbulent medium, in which they form (e.g. Padoan & Nordlund 2002; Hennebelle & Chabrier 2008; Hopkins 2012; Hennebelle & Chabrier 2013). In these models, both the CMF and IMF peaks are set by the “sonic mass”  $M_{\text{sonic}}$ , namely the turbulent Jeans or Bonner-Ebert mass at the sonic scale ( $R_{\text{sonic}}$ ) below-which the turbulence becomes sub-sonic and therefore fails to generate large fluctuations (which seed fragmentation). The critical mass is

$$M_{\text{crit,S}} = M_{\text{sonic}} \sim \frac{2c_s^2 R_{\text{sonic}}}{G}, \quad (3)$$

where  $R_{\text{sonic}}$  is defined through the linewidth-size relation

$$\sigma_{\text{turb}}^2(\lambda) = c_s^2 \frac{\lambda}{R_{\text{sonic}}}. \quad (4)$$

In our calculations  $\sigma_{\text{turb}}^2$  is estimated from the simulations when a star particle forms by measuring the velocity dispersion (after subtracting the mean shear) between neighboring particles in a sphere of radius  $\lambda$  (taken to be that which encloses the nearest  $\sim 32$  gas neighbours).

- **Protostellar feedback models:** Although there are a number of ways newly formed stars can regulate star formation, most studies have concluded that at the scale of the



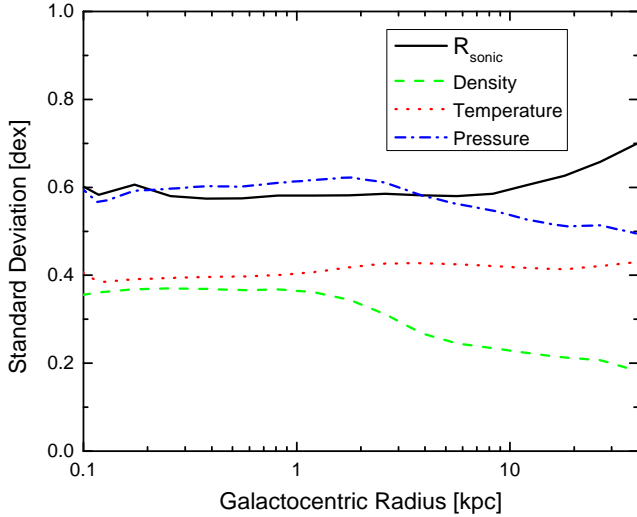


**Figure 5.** Standard deviation in *at formation* star-forming progenitor cloud properties (as in Fig. 3), across the progenitor clouds of all stellar sink particles which reside at a given present-day galacto-centric radius. Note that this is *not* the variation of present day star forming clouds at different radii as progenitor clouds at some present day radius could have formed at wildly different times and positions (for example, at high redshift in a more gas-rich disk with larger pressures and densities). Thermodynamic and turbulent progenitor-cloud properties vary by  $\sim 0.5$  dex at all radii; this implies large IMF variations for any model which has a strong (linear or larger) dependence on these quantities. Example here is from the same galaxy in Fig. 3, but results are very similar across all five simulated galaxies in Table 1.

IMF peak (early protostellar collapse of  $\sim 0.1 M_{\odot}$  clouds) the most important self-regulation mechanism is radiative feedback from protostellar accretion (Bate 2009; Krumholz 2011; Guszejnov et al. 2016). This sets a unique mass and spatial scale within which the protostellar heating has raised the temperature to make the core Jeans-stable, terminating fragmentation. The resulting critical masses are

$$M_{\text{crit,B}} \sim 0.5 \left( \frac{\rho}{1.2 \times 10^{-19} \text{ g/cm}^3} \right)^{-1/5} \left( \frac{L_*}{150 L_{\odot}} \right)^{3/10} M_{\odot}, \quad (5)$$

$$M_{\text{crit,K}} \sim 0.15 \left( \frac{P/k_B}{10^6 \text{ K/cm}^3} \right)^{-1/18} M_{\odot} \quad (6)$$

where  $L_*$  is the average luminosity of accreting protostars and  $P$  is the pressure. These different formulae come from Bate (2009) and Krumholz (2011), respectively; the differences owe to the detailed uncertainties treating radiation. However for our purposes they give *nearly identical* results, so we will focus on the model from Krumholz (2011).

### 3 RESULTS AND DISCUSSION

Fig. 5 shows that there is significant variation the properties of the progenitor GMC complexes which formed stars that ultimately end up at a specific galacto-centric radius. We stress that this is not the variation of properties in *present-day* star-forming clouds, but includes all variations in time as well: if the galaxy progenitor was gas-rich (gas fraction  $\sim 1/2$ ) at  $z \sim 1-2$  for example, then the midplane gravitational pressure ( $\sim G \Sigma_{\text{gas}}^2$ ) could be a factor  $\sim 100$  larger than in the

galaxy today. Fig. 6 shows that this, in turn, produces large IMF variations in all models here except those accounting for protostellar heating. These variations ( $> 0.5$  dex in  $M_{\text{turnover}}$ ) appear strongly ruled-out by observations (Bastian et al. 2010). Note that these results are robust to variations in simulation parameters (see Table 1).

The variations in the IMF predicted by some of the simple models here (e.g. the Jeans-mass models) have often been substantially underestimated in previous work in the literature. In analytic models of the IMF (see references in § 1) or galaxy-scale models which fail to resolve individual “parent clouds”, but post-process the entire galaxy (with  $> \text{kpc}$ -scale resolution) to determine an IMF (Narayanan & Davé 2012; Hopkins 2013; Blancato et al. 2016), it is commonly assumed that all star-forming clouds are uniformly at the same isothermal temperature (e.g.  $T = 10 \text{ K}$  at all densities), virial parameter, and/or lie exactly on the same linewidth-size relation. If the gas at all densities were exactly isothermal, then the variation in the IMF for the opacity-limited EOS models vanishes (all clouds and cores lie on exactly one adiabat). This assumption is not correct, however, as both GMC temperature and virial parameters vary substantially (Larson 2005; Bergin & Tafalla 2007; Nishimura et al. 2015). Similarly, Hopkins (2013) assumed all clouds were isothermal and – within the same galaxy – lie exactly on the same linewidth-size relation (without scatter of systematic variation): this produces zero scatter in  $R_{\text{sonic}}$  or  $M_{\text{sonic}}$ .

Our cloud properties (used to model the IMF) are measured at a density scale of  $\sim 1000 \text{ cm}^{-3}$  and mass scale  $\sim 7000 M_{\odot}$ . Obviously the clouds must continue to evolve, and fragment, to form actual stars – this is what our cloud-scale IMF models attempt to model. One might wonder, however, whether during this process some of the scatter might be reduced (if, for example, the clouds converged to the same temperature). In the opacity-limited models, the equation of state (EOS) is specified (generally the cloud cools with  $T \propto \rho^{-0.3}$  to some density, becomes approximately isothermal, then becomes adiabatic above the opacity-limit density), so this is already built into the model explicitly. In the “Jeans Mass” or “Turbulent/Sonic Mass” models, we have implicitly assumed an isothermal EOS within each cloud. More realistically, let us assume star formation occurs above some critical density  $\rho_{\text{crit}}$  and the gas follows a polytropic EOS with index  $\gamma$ . The critical mass (Table 1) will then depend on  $T_{\text{crit}}(\rho = \rho_{\text{crit}}) = T_{\text{cloud}}(\rho_{\text{crit}}/\rho_{\text{cloud}})^{\gamma-1}$ , as  $M_{\text{crit}} \propto T_{\text{crit}}^{\alpha}$  where  $\alpha = 3/2, 1$  for the Jeans and Turbulent/Sonic models, respectively. Some simple algebra then gives us logarithmic variance in  $M_{\text{crit}}$ ,  $S_{\log M_{\text{crit}}} = \alpha(S_{\log T_{\text{cloud}}} + [\gamma - 1]S_{\log \rho_{\text{cloud}}})$ . Putting in the actual values (Fig. 5) this gives a dispersion  $\sigma_{\log M_{\text{crit}}} \approx 0.6, 0.4$  dex for the Jeans and Turbulent/Sonic models (for any  $\gamma \sim 0.5 - 1.5$ ). This reduces the predicted IMF variation, but still leaves it far larger than observed.

### 4 CONCLUSIONS

In this paper we explore broad classes of IMF models applied independently to a high-resolution fully-cosmological galaxy simulation in order to find the resulting scatter in the IMF. Molecular clouds at a chosen present day location might have formed at very different times and places: only by us-

Model	$M_{\text{crit}}$	Reference	Galactic IMF variation ( $\sigma_{M_{\text{crit}}}$ ) [dex]				
			m12i	m12i	m12i+MHD	m12f	m12m
			(56000 $M_{\odot}$ ) (100 $\text{cm}^{-3}$ )	(7000 $M_{\odot}$ ) (1000 $\text{cm}^{-3}$ )	(7000 $M_{\odot}$ ) (1000 $\text{cm}^{-3}$ )	(7000 $M_{\odot}$ ) (1000 $\text{cm}^{-3}$ )	(7000 $M_{\odot}$ ) (1000 $\text{cm}^{-3}$ )
Jeans Mass	$\propto T^{3/2} \rho^{-1/2}$	Bate & Bonnell 2005	0.60	0.54	0.61	0.56	0.65
Turbulent/Sonic Mass	$\propto TR_{\text{sonic}}$	Hopkins 2012	0.91	0.96	0.86	0.91	0.84
Opacity-limited, $\rho_{\text{crit}}$	$\propto T^{3/2}$	Jappsen et al. 2005	0.63	0.53	0.58	0.54	0.61
Opacity-limited, $\Sigma_{\text{crit}}$	$\propto T^2$	Bate 2009	0.81	0.70	0.75	0.73	0.81
Protostellar Heating	$\propto (\rho T)^{-1/18}$	Krumholz 2011	0.030	0.026	0.031	0.027	0.031

**Table 1.** Rows: Different IMF models compared in this paper, each with the predicted scaling of the IMF turnover mass  $M_{\text{crit}}$  with initial parent cloud properties (§ 2.2), reference, and the predicted  $1\sigma$  dispersion in  $\log_{10}(M_{\text{crit}})$  across the galaxy at present-day (averaging Fig. 5 over all galacto-centric radii). We measure  $\sigma_{M_{\text{crit}}}$  from five simulations: galaxies **m12i**, **m12f**, and **m12m** are three distinct Milky Way-mass ( $\sim 10^{12} M_{\odot}$ ) halos which produce similar disk-like, Milky Way-like galaxies (stellar mass  $\sim 0.5 - 1 \times 10^{11} M_{\odot}$ ), but have different formation histories (see Hopkins et al. 2017 for details). For each we label the mass resolution (in  $M_{\odot}$ ) and minimum density  $n_{\text{crit}}$  for creation of stellar sink particles. For **m12i**, we compare two alternative runs: one at lower resolution, and one including magnetic fields (**m12i+MHD**). The predicted IMF variation is remarkably robust across all these simulations.

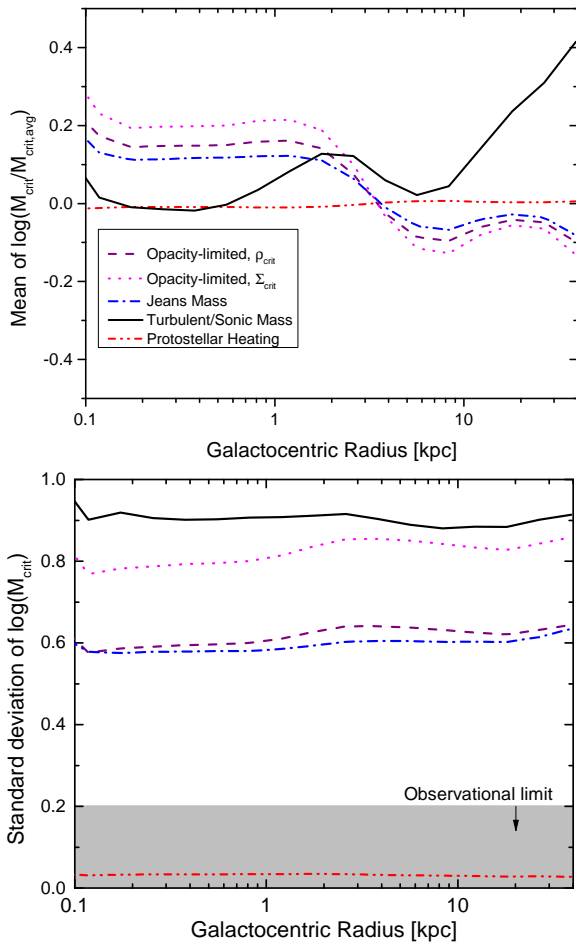


**Figure 6.** Mean (top) and standard deviation (bottom) of the IMF turnover mass  $M_{\text{crit}}$  normalized its galactic average ( $M_{\text{crit,avg}}$ ) at different galacto-centric radii. We compare the IMF models in Table 1, and the observationally allowed range of scatter in the IMF across the Milky Way, from Bastian et al. (2010). Only models accounting for protostellar heating avoid strongly over-predicting the scatter in MW IMFs. The models are shown here for the same example galaxy in Fig. 5, but we obtain very similar results for each of the five simulated galaxies in Table 1.

ing a cosmological simulation instead of local simulations or observations can we properly determine their at-formation properties and infer the IMF variation predicted by different models.

In summary, we find that only models accounting for protostellar heating produce sufficiently weak IMF variations to be compatible with observations. This discrepancy is not apparent in many studies (either analytic or idealized single-cloud simulations) as they artificially assume all clouds begin with the same isothermal temperature and/or linewidth-size relation, while observations consistently find variations in cloud temperatures and velocity dispersions very similar to those in our simulation (Nishimura et al. 2015)<sup>3</sup>. Even if temperature variations are neglected, in the “Turbulent/Sonic Mass” models the turnover mass is proportional to the *square* of the deviation ( $(\sigma_{\text{cloud}}/\langle\sigma[R]\rangle)^2$ ) of each cloud from the linewidth-size relation (Hopkins 2012; Hennebelle & Chabrier 2008), but these deviations are observed to be  $\sim 0.3 - 0.5$  dex (Bolatto et al. 2008) implying  $> 0.6$  dex scatter. Likewise the density dependence in “Jeans Mass” models predicts  $> 0.3$  dex scatter even if all temperature variations are neglected.

The protostellar heating models actually predict IMF variations significantly below the observational limit (see Fig. 6). The variance observed may come from a combination (a) stochastic statistical sampling effects (see Bastian et al. 2010; these may be especially important in small clouds such as Taurus which are not resolved by our simulations, see Kraus et al. 2017), (b) measurement uncertainties, or (c) additional physics not accounted for by the model (e.g. bursty accretion or other physics may modify the radiative efficiency and heating effects of protostars, introducing some IMF variation).

In future work, we will examine whether the protostellar heating models favored in this study produce observably-large IMF variation under more extreme conditions. Preliminary comparison of single-cloud conditions in Guszejnov et al. (2016) suggests these models can produce as much as

<sup>3</sup> Note that Nishimura et al. (2015) only focuses on Orion A and B so these results are not necessarily representative of the entire MW. Also, as we had  $n_{\text{crit}} = 100 \text{ cm}^{-3}$  the average temperature of the progenitor clouds is higher than the observed GMCs as they did not reach the cool, high density phase (see Fig. 3).

factor  $\sim 2$  shifts in the turnover mass under extreme starburst conditions analogous to Arp220, but this needs to be explored in more detail. We will also explore in more detail IMF shape variations, the predicted IMF in different sub-regions of the galaxy (e.g. the galactic nucleus), and the IMF in specific populations (e.g. metal-poor globular clusters versus present-day stellar populations).

## ACKNOWLEDGMENTS

Support for PFH, DG, and XM was provided by an Alfred P. Sloan Research Fellowship, NASA ATP Grant NNX14AH35G, and NSF Collaborative Research Grant #1411920 and CAREER grant #1455342. Numerical calculations were run on the Caltech compute cluster “Zwicky” (NSF MRI award #PHY-0960291) and allocation TG-AST130039 granted by the Extreme Science and Engineering Discovery Environment (XSEDE) supported by the NSF.

## REFERENCES

- Andrews J. E., et al., 2013, *ApJ*, **767**, 51  
 Andrews J. E., et al., 2014, *ApJ*, **793**, 4  
 Bastian N., Covey K. R., Meyer M. R., 2010, *ARA&A*, **48**, 339  
 Bate M. R., 2009, *MNRAS*, **392**, 1363  
 Bate M. R., Bonnell I. A., 2005, *MNRAS*, **356**, 1201  
 Baugh C. M., Lacey C. G., Frenk C. S., Granato G. L., Silva L., Bressan A., Benson A. J., Cole S., 2005, *MNRAS*, **356**, 1191  
 Bekki K., 2013, *ApJ*, **779**, 9  
 Bergin E. A., Tafalla M., 2007, *ARA&A*, **45**, 339  
 Blancato K., Genel S., Bryan G., 2016, preprint, ([arXiv:1612.05658](https://arxiv.org/abs/1612.05658))  
 Bolatto A. D., Leroy A. K., Rosolowsky E., Walter F., Blitz L., 2008, *ApJ*, **686**, 948  
 Brown T. M., et al., 2012, *ApJ*, **753**, L21  
 Cappellari M., et al., 2012, *Nature*, **484**, 485  
 Chabrier G., 2003, *PASP*, **115**, 763  
 Chabrier G., 2005, in Corbelli E., Palla F., Zinnecker H., eds, *Astrophysics and Space Science Library Vol. 327, The Initial Mass Function 50 Years Later*. p. 41  
 Chabrier G., Hennebelle P., Charlot S., 2014, *ApJ*, **796**, 75  
 Conroy C., van Dokkum P. G., 2012, *ApJ*, **760**, 71  
 Davé R., Finlator K., Oppenheimer B. D., 2012, *MNRAS*, **421**, 98  
 Dobbs C. L., et al., 2014, *Protostars and Planets VI*, pp 3–26  
 Ferland G. J., et al., 2013, *Rev. Mex. Astron. Astrofis.*, **49**, 137  
 Ferreras I., Weidner C., Vazdekis A., La Barbera F., 2015, *MNRAS*, **448**, L82  
 Fumagalli M., da Silva R. L., Krumholz M. R., 2011, *ApJ*, **741**, L26  
 Geha M., et al., 2013, *ApJ*, **771**, 29  
 Glover S. C. O., Mac Low M.-M., 2007, *ApJS*, **169**, 239  
 Guszejnov D., Hopkins P. F., 2016, *MNRAS*, **459**, 9  
 Guszejnov D., Krumholz M. R., Hopkins P. F., 2016, *MNRAS*, **458**, 673  
 Hennebelle P., Chabrier G., 2008, *ApJ*, **684**, 395  
 Hennebelle P., Chabrier G., 2013, *ApJ*, **770**, 150  
 Heyer M., Dame T. M., 2015, *ARA&A*, **53**, 583  
 Hopkins P. F., 2012, *MNRAS*, **423**, 2037  
 Hopkins P. F., 2013, *MNRAS*, **433**, 170  
 Hopkins P. F., 2015, *MNRAS*, **450**, 53  
 Hopkins P. F., Quataert E., Murray N., 2012, *MNRAS*, **421**, 3488  
 Hopkins P. F., Narayanan D., Murray N., Quataert E., 2013, *MNRAS*, **433**, 69  
 Hopkins P. F., Kereš D., Oñorbe J., Faucher-Giguère C.-A., Quataert E., Murray N., Bullock J. S., 2014, *MNRAS*, **445**, 581  
 Hopkins P. F., et al., 2017, *MNRAS*, in press [[arXiv:1702.06148](https://arxiv.org/abs/1702.06148)],  
 Hoversten E. A., Glazebrook K., 2008, *ApJ*, **675**, 163  
 Jappsen A.-K., Klessen R. S., Larson R. B., Li Y., Mac Low M.-M., 2005, *A&A*, **435**, 611  
 Koda J., Yagi M., Boissier S., Gil de Paz A., Imanishi M., Donovan Meyer J., Madore B. F., Thilker D. A., 2012, *ApJ*, **749**, 20  
 Kraus A. L., Herczeg G. J., Rizzuto A. C., Mann A. W., Slesnick C. L., Carpenter J. M., Hillenbrand L. A., Mamajek E. E., 2017, preprint, ([arXiv:1702.04341](https://arxiv.org/abs/1702.04341))  
 Kroupa P., 2002, *Science*, **295**, 82  
 Krumholz M. R., 2011, *ApJ*, **743**, 110  
 Krumholz M. R., 2014, *Phys. Rep.*, **539**, 49  
 Larson R. B., 2005, *MNRAS*, **359**, 211  
 Leitherer C., et al., 1999, *ApJS*, **123**, 3  
 Low C., Lynden-Bell D., 1976, *MNRAS*, **176**, 367  
 Luhman K. L., Mamajek E. E., Allen P. R., Cruz K. L., 2009, *ApJ*, **703**, 399  
 Ma X., Hopkins P. F., Wetzel A. R., Kirby E. N., Angles-Alcazar D., Faucher-Giguère C.-A., Keres D., Quataert E., 2016a, preprint, ([arXiv:1608.04133](https://arxiv.org/abs/1608.04133))  
 Ma X., Hopkins P. F., Faucher-Giguère C.-A., Zolman N., Muratov A. L., Keres D., Quataert E., 2016b, *MNRAS*, **456**, 2140  
 Ma X., Hopkins P. F., Feldmann R., Torrey P., Faucher-Giguère C.-A., Keres D., 2017, *MNRAS*,  
 Martín-Navarro I., La Barbera F., Vazdekis A., Ferré-Mateu A., Trujillo I., Beasley M. A., 2015a, *MNRAS*, **451**, 1081  
 Martín-Navarro I., et al., 2015b, *ApJ*, **798**, L4  
 Martín-Navarro I., et al., 2015c, *ApJ*, **806**, L31  
 Masunaga H., Inutsuka S.-i., 2000, *ApJ*, **531**, 350  
 Muratov A. L., Keres D., Faucher-Giguère C.-A., Hopkins P. F., Quataert E., Murray N., 2015, *MNRAS*, **454**, 2691  
 Narayanan D., Davé R., 2012, *MNRAS*, **423**, 3601  
 Narayanan D., Hopkins P. F., 2013, *MNRAS*, **433**, 1223  
 Nishimura A., et al., 2015, *ApJS*, **216**, 18  
 Offner S. S. R., Clark P. C., Hennebelle P., Bastian N., Bate M. R., Hopkins P. F., Moraux E., Whitworth A. P., 2014, *Protostars and Planets VI*, pp 53–75  
 Orr M., et al., 2017, preprint, ([arXiv:1701.01788](https://arxiv.org/abs/1701.01788))  
 Padoan P., Nordlund Å., 2002, *ApJ*, **576**, 870  
 Posacki S., Cappellari M., Treu T., Pellegrini S., Ciotti L., 2015, *MNRAS*, **446**, 493  
 Rice T. S., Goodman A. A., Bergin E. A., Beaumont C., Dame T. M., 2016, *ApJ*, **822**, 52  
 Salpeter E. E., 1955, *ApJ*, **121**, 161  
 Sonnenfeld A., Treu T., Marshall P. J., Suyu S. H., Gavazzi R., Auger M. W., Nipoti C., 2015, *ApJ*, **800**, 94  
 Sparre M., Hayward C. C., Feldmann R., Faucher-Giguère C.-A., Muratov A. L., Keres D., Hopkins P. F., 2015, preprint, ([arXiv:1510.03869](https://arxiv.org/abs/1510.03869))  
 Treu T., Auger M. W., Koopmans L. V. E., Gavazzi R., Marshall P. J., Bolton A. S., 2010, *ApJ*, **709**, 1195  
 Weidner C., Ferreras I., Vazdekis A., La Barbera F., 2013, *MNRAS*, **435**, 2274  
 Weisz D. R., et al., 2015, *ApJ*, **806**, 198  
 Wetzel A. R., Hopkins P. F., Kim J.-h., Faucher-Giguère C.-A., Keres D., Quataert E., 2016, preprint, ([arXiv:1602.05957](https://arxiv.org/abs/1602.05957))  
 Whitworth A. P., Boffin H. M. J., Francis N., 1998, *MNRAS*, **299**, 554  
 Wiersma R. P. C., Schaye J., Smith B. D., 2009, *MNRAS*, **393**, 99  
 van Dokkum P. G., Conroy C., 2010, *Nature*, **468**, 940  
 van Dokkum P. G., Conroy C., 2011, *ApJ*, **735**, L13  
 van de Voort F., Quataert E., Hopkins P. F., Keres D., Faucher-Giguère C.-A., 2015, *MNRAS*, **447**, 140